H-MODE PHYSICS STUDIES ON TCV SUPPORTED BY THE EUROFUSION PEDESTAL DATABASE

B. LABIT, S. CODA, B. P. DUVAL, A. MERLE, L. PORTE, O. SAUTER, U. SHEIKH
École Polytechnique Fédérale de Lausanne (EPFL), Swiss Plasma Center (SPC)
Lausanne, Switzerland
Email: benoit.labit@epfl.ch

M. DUNNE
Max-Planck-Institut für Plasmaphysik
Garching, Germany

L. FRASSINETTI
Division of Fusion Plasma Physics, KTH Royal Institute of Technology
Stockholm, Sweden

R. SCANNELL
CCFE, Culham Science Centre
Abingdon, United Kingdom

TCV TEAM*

EUROfusion MST1 TEAM†

Abstract

The paper is an overview of the H-mode physics studies on TCV. Historically, ELMy H-modes were obtained with ohmic heating only (q95<3). With the installation of a X3 ECRH system, the operational range increased to low pedestal collisionalities, in the ITER range, allowing pedestal pressures to increase by a factor 3-4. In 2015, a neutral beam injector (H or D) was installed and H-modes at q_{95}>3 are now routinely obtained. The pedestal database developed for EUROfusion is presented and used within the paper.

1. INTRODUCTION

The H-mode confinement regime is projected to be the main operational scenario on ITER [1] and the current foreseen scenario for a fusion reactor. A continuous effort towards better predictive capabilities of H-mode confinement is being pursued on both experimental and theoretical fronts. The H-mode is characterised by the formation of a pedestal near the plasma edge and, as the fusion power scales as p_{ped}^2, it is advantageous to maintain a high pedestal pressure. While the pedestal temperature is well predicted by the EPED model [2], a model for the particle transport across the pedestal is still missing. Operations with large pedestal pressures are challenged by the need to mitigate H-mode characteristic Type-I ELMs either by creating a highly radiating divertor using impurity injection [3] or by developing and controlling ELM-free or small ELMs regimes [4]. With a pedestal database (Section 2), H-mode physics studies performed on TCV are reviewed with emphasis on comparisons between historically ECRH dominated scenario (Section 3) and recent NBH H-mode regimes (Section 4). Finally, preliminary results of the first isotope studies on ELMy H-mode are presented in Section 5.

2. THE PEDESTAL DATABASE

The TCV pedestal database is one of several databases promoted by EUROfusion to stimulate multi-machine comparisons, (JET, AUG, MAST-U and TCV), with common parameter definitions [5, 6] and a common platform (IMAS: ITER integrated modelling and analysis suite). The primary diagnostic for pedestal parameters is Thomson Scattering (TS) [7, 8] that measures the profiles of electron temperature (T_e) and density (n_e). The

* See author list of S. Coda et al 2019 Nucl. Fusion 59 112023

† See author list of B. Labit et al 2019 Nucl. Fusion 59 086020

pedestal structure is determined from the pre-ELM temperature and density composite profiles (75-90% of the ELM cycle) as shown in Figure 1a-b) where 5 TS profiles are used to construct the composite profiles.

Pedestal parameters are obtained using a *mtanh fitting* function [9] $\frac{h_1-h_0}{2}\left(\frac{(1+sx)e^x-e^{-x}}{e^x+e^{-x}}+1\right)+h_0$ with $x=\frac{p-\rho_\psi}{(w/2)}$ where $\rho_\psi=\sqrt{\psi_N}=\sqrt{\frac{\psi-\psi_0}{\psi_a-\psi_0}}$ is the normalised radial coordinate, h_1 and h_0 the pedestal height and offset in the scrape-off layer (SOL), s the slope inside the pedestal top, p the pedestal position and w the pedestal width. To reduce uncertainties from the equilibrium reconstructions, temperature and density profiles were systematically displaced (<2% of ρ_ψ on average) such that T_e^{sep}=50 eV, estimated using the two-point model for

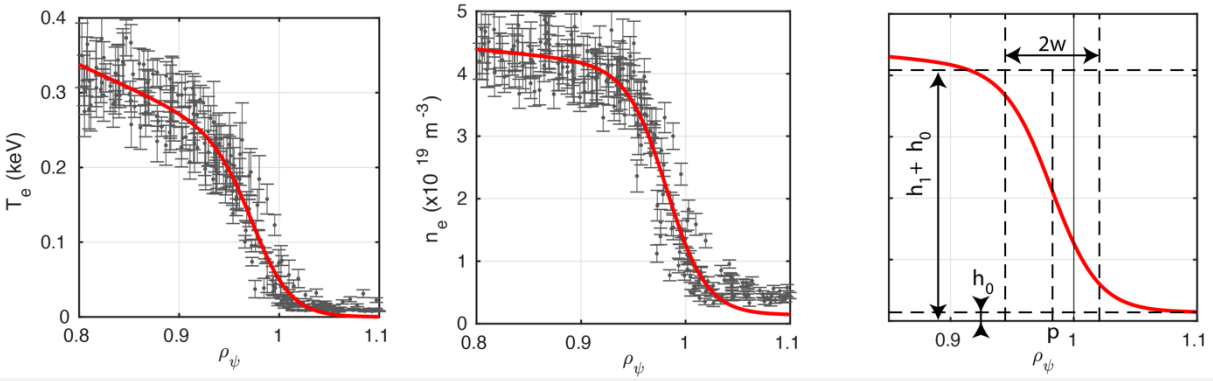

FIG 1 : Example of the composite profiles for #66347 (a) for the temperature and (b) the density. The pre-ELM profiles have been selected in stationary phase 1 s long; c). Example of the mtanh fitting function with the various fit parameters.

the power balance at the separatrix. To enhance the overall pedestal data quality, entries were selected according to following rules: steady state intervals over at least 0.4s (~10τ_E) and a reduced R^2 for the fit in the region $0.8<\rho_\psi<1.05$ larger than 0.75.

The TCV pedestal database currently contains ~750 entries of about 170 parameters. 90% of the entries are with nominal toroidal magnetic field B_0=1.4T and all with lower single-null plasmas with the ∇B-drift towards the X-point (favourable configuration). The plasma current was varied between 140 kA (q_{95}=5.2) and 420 kA (q_{95}=2.1). The plasma shaping capabilities of TCV have been exploited to cover the range of parameters: $1.3<\kappa<1.8$, $0.2<\delta_b<0.8$ and $-0.3<\delta_u<0.8$.

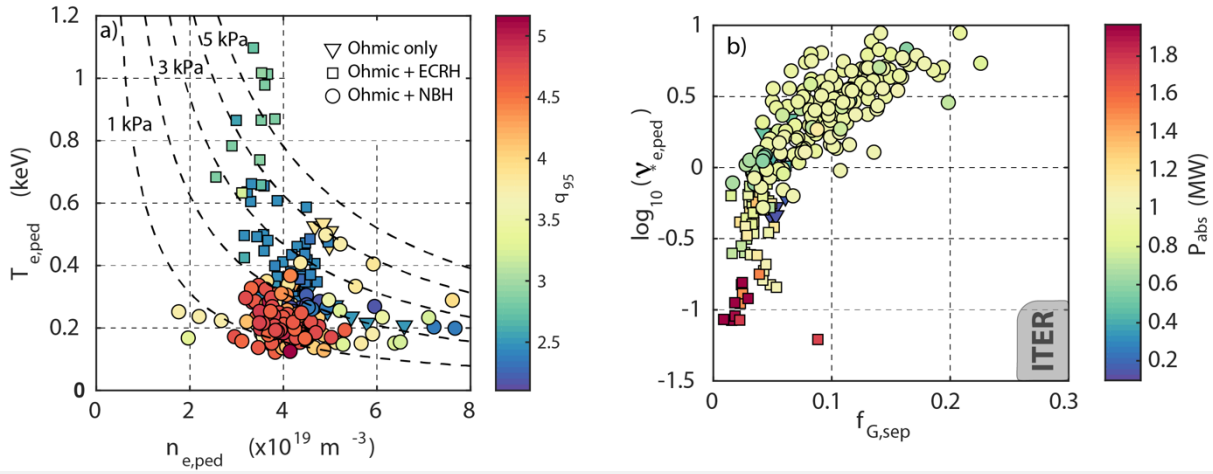

FIG 2 : a) Pedestal top temperature vs pedestal top density for the 3 heating scenarios applied, color-coded with q_{95}; b). Pedestal electron collisionality vs plasma density at the separatrix normalised to Greenwald density color-coded with the total absorbed power.

An overview of the database is shown in Figure 2. For all TCV's heating methods, (Ohmic, ECRH and NBH), the pedestal temperature is shown as a function of the pedestal density (Fig. 2a)). With ECRH, the density range is quite narrow (X2 cutoff) but $T_{e,ped}$>0.7 keV is achieved with central X3 and edge X2 heating. With NBH, high densities can be obtained permitting detachment studies with nitrogen seeding experiments. Figure 2b) shows a view including the projected region of ITER operations. Collisionality is here defined as $\nu_{*e}^{ped}=6.921.10^{-18}\ln\Lambda\frac{Rq_{95}n_e^{ped}}{\varepsilon^{3/2}\left(T_e^{ped}\right)^2}$ with $\ln\Lambda=31.3-\ln\frac{\sqrt{n_e^{ped}}}{T_e^{ped}}$ with ε=a/, the density is in m^{-3}, the temperature in eV and

$f_G^{sep} = \frac{n_e^{sep}}{n_G}$ where n_e^{sep} is the separatrix density estimated from pedestal fit normalised to $n_G = \frac{I_p}{\pi a^2}$, the Greenwald fraction. Although both parameters can reach values close that for ITER, they cannot be achieved simultaneously. Indeed, in today's tokamaks, pedestal collisionalities relevant for ITER (ν_*^{ped}<0.1) may be achievable with an ECRH H-mode operational regime but conditions for partial detachment, f_G^{sep} ~0.4 at the separatrix, are not possible at the same time.

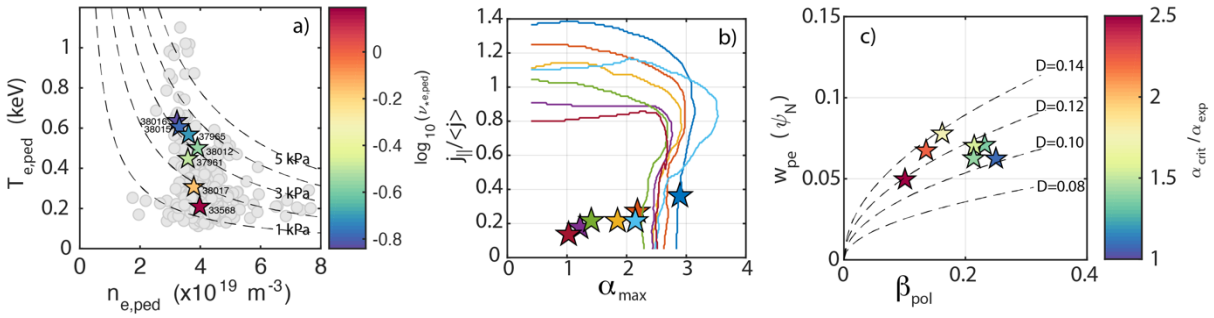

FIG 3 : (a) Pedestal temperature vs pedestal density of the selected shots from the collisionality scan; (b). Experimental values of the normalised current density vs the normalised pressure gradient (stars). The solid lines indicate the peeling-ballooning boundary; c) Pressure pedestal width vs poloidal beta estimated at the pedestal top. The color coding indicates the proximity to the PB boundary.

3. H-MODE SCENARIOS WITH DOMINANT ELECTRON HEATING

3.1. Summary of past results

H-mode plasmas with Type-III ELMs are achieved in TCV with Ohmic heating only for q_{95}<3. Here, core plasma density is too high for 2nd harmonic ECRH, but central heating at the third harmonic (X3) is possible. As the injected X3 power is increased (0<P_{X3}<0.5 MW), the type-III ELM frequency decreases to f_{ELM}~50Hz. Additional X3 power doesn't change the ELM frequency but increases significantly the normalised lost energy per ELM (ΔW/W~17%) (see section 3.3). Finally, for P_{X3}>0.8MW, the ELM frequency increases, signifying Type-I ELMs, with a simultaneous decrease in the normalised ELM losses [7, 10, 11]. Typical pedestal values for an ELMy H-mode heated with 1 MW of ECRH are T_e^{ped}~0.8 keV, n_e^{ped} ~3x10^{19}m^{-3}, n_e^{sep}~0.2n_e^{ped} and $T_e(0)/T_i(0)$~6. Using the pedestal Thompson spectrometers [7], the temporal evolution of electron density and temperature profiles was investigated during H-mode phases with ELMs of type I and type III [10, 11]. The pedestal pressure gradient sometimes saturates shortly before the ELM onset and the maximum pressure gradients predicted by ideal MHD stability calculations were in good agreement with experimental observations for a range in plasma edge collisionalities. At low collisionality, for type I ELMs, the pressure gradients are limited by low- to medium-*n* kink-ballooning modes (see section 3.2). The measurements also revealed a small, but significant, variation of the pedestal position with respect to the separatrix during the ELM cycle.

Such hot plasmas at low densities for ρ_ψ>0.8, including the pedestal, are still accessible for X2 heating (T_e^{ped}>0.8 keV in Fig2a). Contol of the ELM frequency by ECRH modulation has been demonstrated [12] where weak shaping was employed (δ<0.2) so the confinement was not optimised and probably where type-III were destabilised (f_{elm}>300Hz, ΔW/W~5%). The same scenario was used to investigate the H-mode properties for a snowflake (SF+) divertor configuration where the ELM frequency was reduced by a factor up to 3 while ΔW/W only increased by 20%-30% compared to an identically shaped, conventional, single-null diverted H mode [13]. Interestingly, a quasi-stationary ELM-free regime was obtained with 1.2 MW of X3 power for unfavourable ∇B configurations [14]. These H-modes operated at β_N~2, f_G~0.25 with high energy confinement (H_{98y2} ~1.6). Surprisingly, this scenario featured a strong density peaking factor and spontaneous toroidal momentum in the co-current direction.

3.2. Pedestal collisinality and closeness to the peeling-ballooning boundary

In this section, a scan in collisionality is discussed together with the analysis workflow used in the database. A set of pedestals from plasmas with q_{95}=2.5, B_0=1.4 T, δ=0.45, κ = 1.7, 0<P_{ECH}<0.8 MW, 4<n_{el}<5x10^{19} m^{-3} was selected (Fig.3a). Pressure profiles are fitted (*mtanh* for the pedestal, 4th order polynomial for the core) and used to constrain a new plasma equilibrium reconstruction using the CHEASE code. The bootstrap current is computed using the Sauter's formulas [15]. The normalised current density $j_{\parallel}/\langle j\rangle$ and the normalised pressure gradient $\alpha = -\frac{\partial_\psi V}{(2\pi)^2}\left(\frac{V}{2\pi^2 R}\right)^{1/2}\mu_0 p'$ are evaluated at the pedestal position and represented by stars in Fig. 3b). Within the framework of ideal MHD, the stability limits for ballooning and external kink modes are obtained from the suite of codes BALM/KINX [16], using fitted pressure profiles, where the peeling-ballooning (PB) boundary is then determined (solid lines in Fig. 3b)). Graphically, from Fig.3b), it is clear that the pedestal moves closer to the PB boundary as the collisionality decreases, eventually reaching it for the lowest ν_*^{ped} value. To quantify the agreement between the experimental pedestals and the PB model, a similar approach explained in [6] is used: a self-consistent path in the j–α space is determined by increasing the height of the pedestal temperature and then self-consistently calculating the current profile. This is repeated until the marginally stable pedestal temperature height is reached and the critical normalized pressure gradient (α_{crit}), normalized current density (j_{crit}) and pedestal temperature ($T_{e,crit}$) are identified from the intersection of this path with the PB boundary. In Fig.3c), the pedestal pressure width $w_{p_e}^{EPED} = \frac{w_{T_e}+w_{n_e}}{2}$ is shown as a function of the poloidal beta at the pedestal $\beta_\theta^{ped} = \frac{p_e^{ped}}{B_\theta^2/(2\mu_0)}$. It has to be noted that only the electron pressure is used in this definition. Indeed, T_i measurements were very scarce for H-mode with dominant ECRH since the DNBI path (Z_{DNBI}=0 cm) barely intercepted the plasma (Z_{mag}=23cm). At the beginning of the scan, the pedestal width increases with ν_*^{ped} decreases, indicative of an increased transport whereas, at larger β_θ^{ped} (low ν_*^{ped}), the pedestal shrinks again. For $\alpha_{crit}/\alpha_{exp}$~1, the pedestal width approaches w_{pe}=0.1$(\beta_\theta^{ped})^{1/2}$ which is close to the dependency found on AUG.

3.3. Large ELMs regime with coupling with core MHD

For H-mode with dominant electron heating, the scenario with the better confinement (H_{98y2}~1.1) features low frequency large ELMs (losses up to 20% with 1MW of ECRH) [11]. This is illustrated in Fig4.a) where 5 shots with a range of EC power are highlighted, the main other parameters remaining unchanged (q_{95}=2.5, B_0=1.4T, δ=0.45, κ = 1.7). With increased EC power, the pedestal pressure increases from 2 kPa to 4 kPa (Fig. 5b) while its width doesn't vary significantly (Fig. 4c). For the largest EC power, the pedestal is very close to the

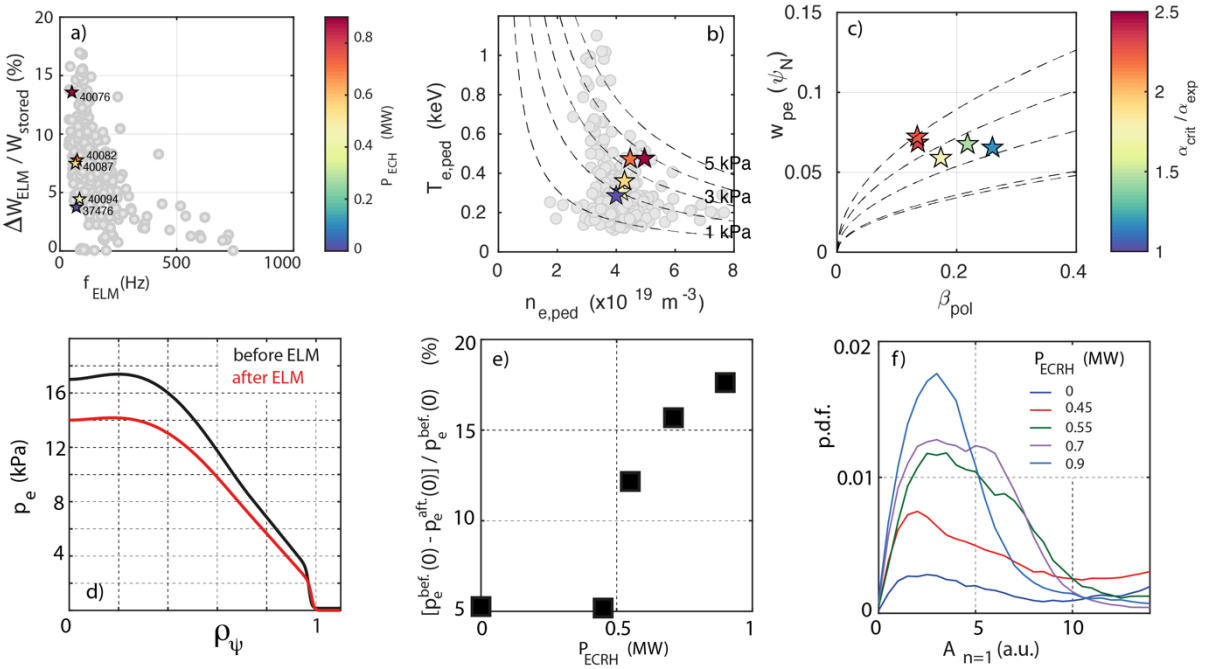

FIG 4 : a) Fraction of loss energy vs ELM frequency for the entire database. The shots from the power scan are highlighted; b) Pedestal temperature vs pedestal density; c) Pedestal pressure width vs poloidal beta; d) Pressure profiles for #40076; e) Relative amplitude of the pressure loss in the plasma centre vs absorbed ECRH power; f)

PB boundary and the transport coefficient D close to 0.1. Fig. 4d), plots the ensemble averaged pressure profile before and just after an ELM crash (#40076, P_{ECRH}=0.9MW). The ELM crash affects the entire profile leading to intolerable pressure losses (Fig. 4e). A possible explanation would be the existence of a coupling between the ELM instability with core MHD modes (m/n=1/1). Indeed, it is seen that not only does the likelihood of a n=1 mode increase with power, but also its amplitude (Fig. 5g). Transport modelling would be required to confirm this conjecture.

4. H-MODE WITH DOMINANT ION HEATING

4.1. Summary of main results

An H-mode operational extension towards high pedestal and higher separatrix densities has become possible with neutral beam heating (1.3 MW, 25 keV), in operation since 2015. Moreover, ELMy H-mode can now be achieved at lower plasma current (q_{95}>3) allowing the development of an ITER baseline scenario on TCV (q_{95}~3-3.6, κ=1.7, δ=0.4) [17]. A starting scenario at q_{95}~4.5, κ=1.5, δ=0.4-0.5 is well established accompanied by Type-I ELMs (f_{ELM}~100 Hz, ΔW/W~10%) and typical pedestal parameters T_e^{ped}~0.2 keV and n_e^{ped}~4x10^{19} m^{-3}. The effects of D2 fuelling and N2 seeding on the pedestal stability and plasma confinement were investigated. Both induce an outward shift of the pedestal density relative to the pedestal temperature with a corresponding outward shift of the pedestal pressure that, in turn, reduces the peeling-ballooning stability, degrades the pedestal confinement, and reduces the pedestal width [18], in line with AUG and JET results [19]. A small ELM regime with high confinement was achieved for sufficiently high separatrix density and the magnetic configuration was close to a double null (δ>0.4) [20]. A regime extension to q_{95}<4 was recently achieved (see section 4.2).

In 2019, TCV was operated with a baffled divertor primarily to better understand the physics of detachment [21]. The effect of a closed divertor on above H-mode scenario at q95=4.7 was investigated [22]. The role of plasma fuelling and nitrogen seeding were, in particular, expected to change compared to the open divertor. It was observed that p_e^{ped}=1.5 kPa can be maintained at divertor neutral pressures increased by a factor of 4. Remarkably, good confinement (H_{98y2}~1) was maintained even though the total radiated power increased by a factor of 3, indicating that the baffled divertor upgrade has improved divertor performance whilst maintaining core performance. A reduction in p_e^{ped} with an outward shift in the density pedestal position was reported for all discharges [22]. Nevertheless, the baffled divertor upgrade reduced the outward shift at high divertor neutral pressures and was thus able to maintain higher p_e^{ped}. This is illustrated in Fig5b) where higher T_e^{ped} are achieved with baffles (red squares) compared to pedestals from open divertor operation (black squares).

Comparison with the EPED1 model indicated that TCV, like JET, does not follow the scaling $w_{pe}=D(\beta_\theta^{ped})^{1/2}$ with the model parameter related to transport D=0.076. The difference between experimental p_e^{ped} and EPED1

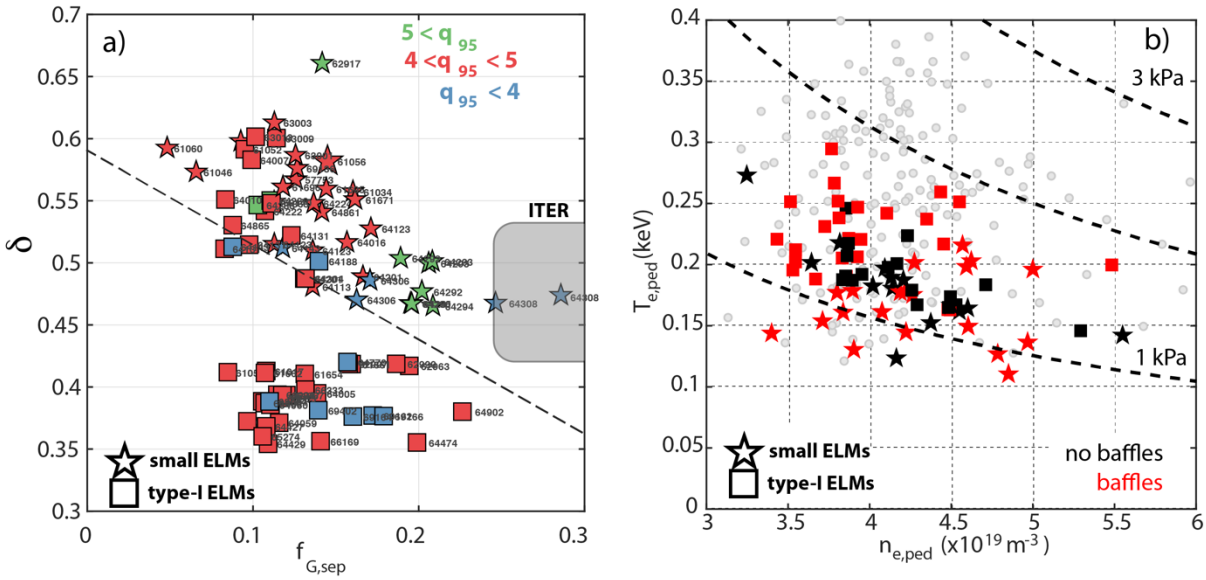

FIG 5 : (a) Operational space for the small ELM regime on TCV: plasma triangularity vs normalised density at the separatrix for small ELMs (stars) and type-I (squares). The small ELM regime has been extended to q95<4. (b). Pedestal temperature vs pedestal density for small ELM regime (stars) compared to type-I cases (squares). Open divertor (black) and closed divertor with baffles (red) are compared.

model predictions was previously partially attributed to a relative shift in the temperature and density pedestal positions [18]. Operation with a baffled divertor did not result in a systematic difference in D.

4.2. Extension of the parameter space for the small ELM regime

The small ELM regime (now called the Quasi-Continuous Exhaust – QCE – regime) has been further investigated in AUG and TCV [23]. Originally, this high confinement regime was achieved if two conditions were simultaneously fulfilled. First, the plasma density at the separatrix must be sufficiently hight ($f_G^{sep} \sim 0.15$), leading to a pressure profile flattening at the separatrix, which stabilises type-I ELMs. Second, the magnetic configuration must be close to a double null (DN), achievable with a high triangularity, leading to a reduction of the magnetic shear in the vicinity of the far separatrix. As a consequence, the stabilising effect on ballooning modes is weakened [20]. During 2019 operation with baffles, the operational space for the small ELM regime was extended, in particular, to $q_{95}<4$ values. This is illustrated by Fig.5a) where the normalised separatrix density and the average triangularity are reported for small ELM plasmas (stars) and compared with type-I cases (squares). The dash-line is there to guide the eye in separating the regimes. The constrains on the triangularity are seen to relax if f_G^{sep} can be increased suggesting that the small ELM regime could be achieved in ITER. Nevertheless, in today's tokamaks the regime is observed only for high collisionalities so an extrapolation to low collisionalities must be demonstrated with modelling. Compared to type-I ELM cases, the pedestal temperature did not systematically increase with baffles inserted for the small regime (Fig. 5b). This may be explained if, at the high fuelling levels used for the small ELM regime, the baffles are no longer separating the divertor and the upstream SOL.

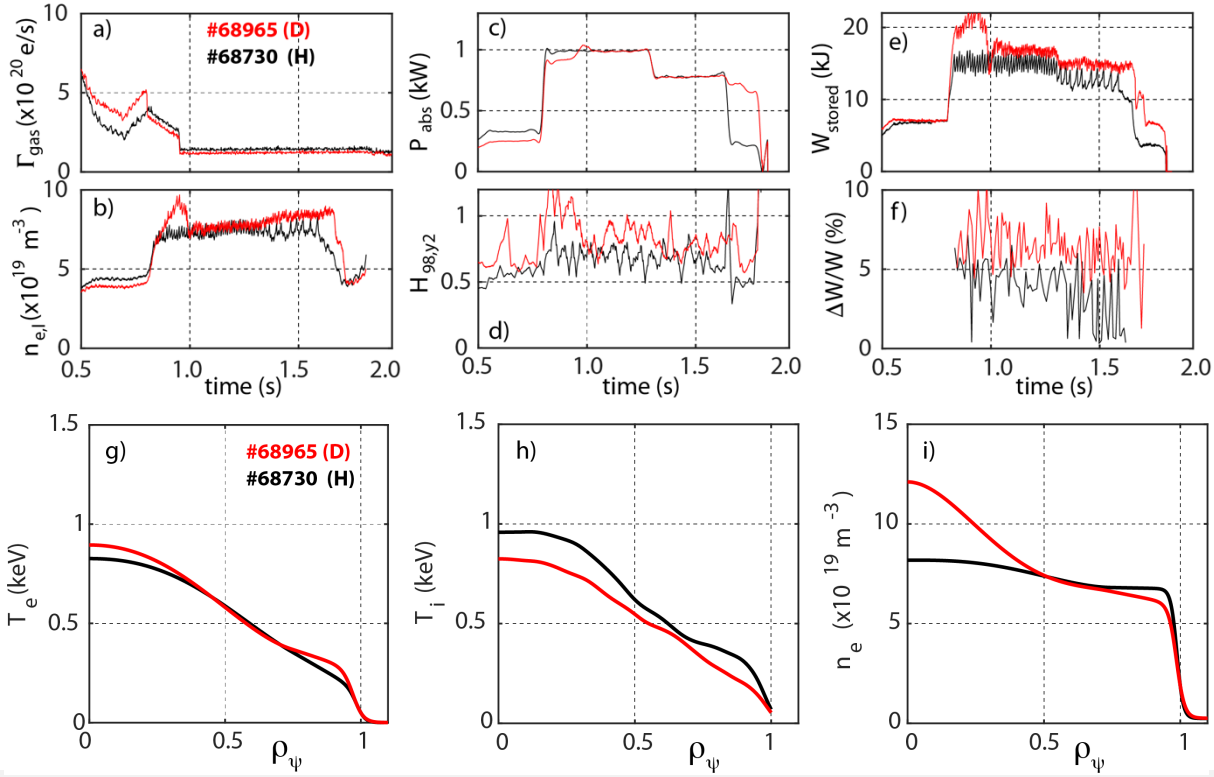

FIG 6 : Comparison of #68730 (H) with #68965 (D) a) Gas fuelling; b) Line averaged density; c) Absorbed power; d) H-mode confinement factor H_{98y2}; e) Stored energy; f) Normalised ELM losses; g) Electron temperature profile; h) Ion temperature profile; i) Electron density profile.

5. TYPE-I ELMY SCENARIO IN HYDROGEN

Recently, and for the first time, a type-I H-mode in hydrogen was obtained on TCV with a Hydrogen neutral beam. Since the pre-fusion high power operation of ITER will preferentially be performed with hydrogen plasmas, it is important to better understand the confinement properties of these plasmas. The main parameters of the scenario are reported in Figure 6 (#68730). A lower-single null diverted configuration was used (κ=1.5, δ=0.4) and a plasma current of 210 kA (q_{95}=3.3) was needed as, at 170 kA (q_{95}=4.7), 1 MW of beam power was insufficient to trigger a L-H transition in H. An accompanying discharge in deuterium is shown for comparison

(#68965). Although this discharge displays NTM behaviour, the confinement is better than for #68730 that was free of MHD modes. While temperature profiles (electron and ion) are reasonably similar, the density profile is much less peaked in H than D. For D plasmas, the density peaking is believed to be a contribution from central fuelling from NBH and from the absence of the drift mode-driven transport [17], so beam fueling may be less important in H plasmas, but a change in particle transport cannot be excluded. A scan in gas fueling and others with impurity seeding (helium or nitrogen) were performed for both scenarios and will be reported in the future.

6. OUTLOOK

The goal of the paper was to present the main features of the TCV pedestal database developed with EUROfusion together with JET, AUG and MAST-U. In addition to the summary of past results on H-mode physics studies on TCV, the database has been used to illustrate the latest achievements. A second neutral beam (1MW, 55keV), planned by the end of 2021, will open new possibilities, not only for H-mode physics at large β_N, but also for fast particle physics. In support of ITER operation preparation, H-mode physics with dominant electron heating will be revisited, in particular with the foreseen upgrade to high power dual-frequencies gyrotrons on TCV. Pedestal transport, in particular for the density, will be further characterised with turbulence diagnostics which are currently begin developed strongly [24]. Experimental turbulence characteristics may then be used for comparison with gyrokinetic nonlinear simulations.

ACKNOWLEDGEMENTS

This work has been carried out within the framework of the EUROfusion Consortium and has received funding from the Euratom research and training programme 2014 - 2018 and 2019 - 2020 under grant agreement No 633053. The views and opinions expressed herein do not necessarily reflect those of the European Commission. This work was supported in part by the Swiss National Science Foundation.

REFERENCES

[1] E.J DOYLE et al., "Chapter 2: Plasma Confinement and Transport, Progress in the ITER Physics Basis", Nucl Fusion **47**, S18 (2007)

[2] P.B SNYDER et al., "A first-principles predictive model of the pedestal height and width: development, testing and ITER optimization with the EPED model" Nucl. Fusion **51** 103016 (2011)

[3] A. KALLENBACH et al., "Partial detachment of high power discharges in ASDEX Upgrade" Nucl. Fusion **55** 053026 (2015)

[4] J. STOBER, et al., "Type II ELMy H-modes on ASDEX Upgrade with good confinement at high density" Nucl. Fusion **41** 1123–34 (2001)

[5] https://users.euro-fusion.org/iterphysicswiki/index.php/Database

[6] L. FRASSINETTI et al., "Pedestal structure, stability and scalings in JET- ILW: the EUROfusion JET-ILW pedestal database", 2021 Nucl. Fusion **61** 016001

[7] R. BEHN et al., " Edge profiles of electron temperature and density during ELMy H-mode in ohmically heated TCV plasmas" *Plasma Phys. Control. Fusion* **49** 1289 (2007)

[8] P. BLANCHARD et al., "Thomson scattering measurements in the divertor region of the TCV Tokamak plasmas" JINST **14** C10038 (2019)

[9] R. GROEBNER et al., "Progress in quantifying the edge physics of the H mode regime in DIII-D", Nucl. Fusion **41** 1789 (2001)

[10] A. PITZCHKE, "Pedestal Characteristics and MHD Stability of H-Mode Plasmas in TCV", PhD thesis, EPFL, no 4917 (2011)

[11] A. PITZCHKE et al., "Electron temperature and density profile evolution during the ELM cycle in ohmic and EC-heated H-mode plasmas in TCV", Plasma Phys. Control. Fusion, **54**, 015007 (2012)

[12] J.X. ROSSEL et al., "Edge-localized mode control by electron cyclotron waves in a tokamak plasma" Nucl. Fusion **52** 032004 (2012)

[13] F. PIRAS et al., « Snowflake H-mode in a tokamak plasma », Phys. Rev. Letters, **105**, 155003 (2010)
[14] L. PORTE et al., "Plasma dynamics with second and third-harmonic ECRH and access to quasi-stationary ELM-free H-mode on TCV," Nucl. Fusion, **47**, 8, 952–960 (2007)
[15] O. SAUTER et al., "Neoclassical conductivity and bootstrap current formulas for general axisymmetric equilibria and arbitrary collisionality regime" Phys. Plasmas **6** 2834 (1999); "Erratum" Phys. Plasmas **9** 5140 (2002)
[16] A. MERLE, et al., "Pedestal properties of H-modes with negative triangularity using the EPED-CH model", Plasma Phys. Control. Fusion, **59**, 10, 104001, 2017.

[17] O. SAUTER et al., "ITER baseline scenario investigations on TCV and comparison with AUG", this conference
[18] U. A. SHEIKH et al., "Pedestal structure and energy confinement studies on TCV," Plasma Phys. Control. Fusion, **61**, 1, 014002 (2019)
[19] L. FRASSINETTI et al., "Role of the pedestal position on the pedestal performance in AUG, JET-ILW and TCV and implications for ITER", Nucl. Fusion, 59, 7 076038 (2019)
[20] B. LABIT et al., "Dependence on plasma shape and plasma fuelling for small edge-localized mode regimes in TCV and ASDEX Upgrade," Nucl. Fusion, **59**, 8 086020 (2019)
[21] C. THEILER et al., "Advances in understanding power exhaust physics with the new, baffled TCV divertor", this conference
[22] U. A. SHEIKH et al., "Impact of the new TCV baffled divertor upgrade on pedestal structure and performance", Nucl. Mat. Energy, **26**, 100933 (2021)
[23] M. FAITSCH et al., "High density, high confinement, power exhaust compatible H-mode regime in TCV and ASDEX Upgrade", this conference
[24] P. A. MOLINA CABRERA et al., "High resolution density pedestal measurements during Edge Localized Modes by short-pulse reflectometry in the TCV tokamak", submitted to Plasma Phys. Control. Fusion